

AD-A080 464

MINNESOTA UNIV MINNEAPOLIS DEPT OF CHEMISTRY
MOLECULAR DIPOLE MODEL FOR THE INTERNAL OPTIC MODES OF SURFACE --ETC(U)
JAN 80 H NICHOLS, R M HEXTER

N00014-77-C-0209

F/G 7/4

UNCLASSIFIED TR-4

NL

[or]
AD
SUBJECT

END
DATE
FILMED
3-80
DA

LEVEL 1

12
SC

OFFICE OF NAVAL RESEARCH

Contract N00014-77-C-0209

Task No. NR 051-642

TECHNICAL REPORT NO. 4

ADA 080464

Molecular Dipole Model for the Internal Optic
Modes of Surface Adsorbed Molecules:
Classical Image Theory

by

Henry Nichols and Robert M. Hexter

DDC
RECEIVED
FEB 9 1980
E

Prepared for Publication

in the

Journal of Chemical Physics

University of Minnesota
Department of Chemistry
Minneapolis, MN

January 21, 1980

Reproduction in whole or in part is permitted for
any purpose of the United States Government

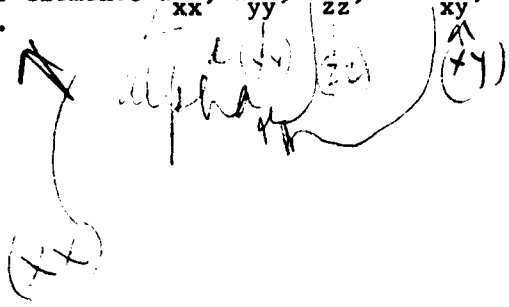
This document has been approved for public release
and sale; its distribution is unlimited

DDC FILE COPY

REPORT DOCUMENTATION PAGE		READ INSTRUCTIONS BEFORE COMPLETING FORM
1. REPORT NUMBER	2. GOVT ACCESSION NO.	3. RECIPIENT'S CATALOG NUMBER 9
4. TITLE (and Subtitle) MOLECULAR DIPOLE MODEL FOR THE INTERNAL OPTIC MODES OF SURFACE ADSORBED MOLECULES: CLASSICAL IMAGE THEORY		5. TYPE OF REPORT & PERIOD COVERED Technical Report, No. 4
7. AUTHOR(s) Henry Nichols Robert M. Hexter		6. PERFORMING ORG. REPORT NUMBER
9. PERFORMING ORGANIZATION NAME AND ADDRESS The Regents of the University of Minnesota Minneapolis, MN 55455		8. CONTRACT OR GRANT NUMBER(s) 15 N00014-77-C-0209
11. CONTROLLING OFFICE NAME AND ADDRESS Chemistry Program Office of Naval Research Arlington, VA 22217		10. PROGRAM ELEMENT, PROJECT, TASK AREA & WORK UNIT NUMBERS 11 22 Jan 80
14. MONITORING AGENCY NAME & ADDRESS (if different from Controlling Office) 14 TR-4		12. REPORT DATE January 21, 1980
		13. NUMBER OF PAGES 42
		15. SECURITY CLASS. (of this report) Unclassified
		15a. DECLASSIFICATION/DOWNGRADING SCHEDULE
16. DISTRIBUTION STATEMENT (of this Report) Approved for public release; distribution unlimited		
17. DISTRIBUTION STATEMENT (of the abstract entered in Block 20, if different from Report)		
18. SUPPLEMENTARY NOTES Preprint, submitted to Journal of Chemical Physics		
19. KEY WORDS (Continue on reverse side if necessary and identify by block number) Surfaces, group theory, dipolar interactions, adsorbed molecules, metal, carbon monoxide on platinum, vibrational selection rules		
20. ABSTRACT (Continue on reverse side if necessary and identify by block number) A molecular dipole model is developed to describe dipolar coupling in surface adsorbed molecules using classical image theory. Only the internal optic modes of the adsorbed molecules are considered. Expanding the dipoles associated with both real and image molecules in terms of the same molecular normal coordinate results in a frequency shift twice that previously expected for dipolar coupling in adsorbed molecules. Application of the model to carbon monoxide adsorbed on platinum indicates that the observed frequency vs.		

233 525 alt

coverage behavior can be attributed to dipolar coupling. The irreducible corepresentations of Shubnikov type II, or grey, groups are used to describe the symmetry and spectroscopic activity of the molecule-plus-image system. Infrared activity is associated only with molecular vibrations having non-zero dipole moment derivative components perpendicular to the surface. Raman activity is associated only with those molecular vibrations having non-zero Raman scattering tensor elements α_{xx} , α_{yy} , α_{zz} , or α_{xy} , where z is perpendicular to the surface.



Accession For	
NTIS (General)	<input checked="" type="checkbox"/>
DDC TAB	<input type="checkbox"/>
Unannounced	<input type="checkbox"/>
Justification	<input type="checkbox"/>
By _____	
Distribution _____	
Availability _____	
Dist.	Availability for special
A	

MOLECULAR DIPOLE MODEL FOR THE
INTERNAL OPTIC MODES OF SURFACE ADSORBED MOLECULES:
CLASSICAL IMAGE THEORY

by Henry Nichols and Robert M. Hexter
Department of Chemistry
University of Minnesota
Minneapolis, Minnesota

ABSTRACT

A molecular dipole model is developed to describe dipolar coupling in surface adsorbed molecules using classical image theory. Only the internal optic modes of the adsorbed molecules are considered. Expanding the dipoles associated with both real and image molecules in terms of the same molecular normal coordinate results in a frequency shift twice that previously expected for dipolar coupling in adsorbed molecules. Application of the model to carbon monoxide adsorbed on platinum indicates that the observed frequency vs. coverage behavior can be attributed to dipolar coupling. The irreducible corepresentations of Shubnikov type II, or grey, groups are used to describe the symmetry and spectroscopic activity of the molecule-plus-image system. Infrared activity is associated only with molecular vibrations having non-zero dipole moment derivative components perpendicular to the surface. Raman activity is associated only with those molecular vibrations having non-zero Raman scattering tensor elements α_{xx} , α_{yy} , α_{zz} , or α_{xy} , where z is perpendicular to the surface.

INTRODUCTION

Pearce and Sheppard have advanced the idea that a metal surface selection rule is operative for the spectroscopic activity of surface adsorbed molecules.¹ In an infrared study of ethylene adsorbed on various silica-supported metals, these authors found that only the vibrational modes having non-zero dipole moment derivative components perpendicular to the surface were infrared active. They explained the observed spectroscopic activity in terms of image dipoles induced in the metal substrate by the adsorbed molecules. A dipole moment change parallel to the surface associated with a vibration of the adsorbed molecule was shown to be canceled by a dipole moment change of the same magnitude, but in the opposite direction, induced in the substrate. Molecular vibrations having dipole moment changes perpendicular to the surface would, however, be infrared active since the image dipole is in the same direction; indeed, for the same reason, the total dipole moment change would be doubled.

Hexter and Albrecht have examined the symmetry properties of the real-image dipole system, where the real dipole is taken throughout this paper to mean the dipole located on the molecule.² The spectroscopic activity of surface adsorbed molecules was analyzed in terms of the irreducible representations of a grey point group describing the symmetry of the real-image dipole system.

In an infrared transmission study of CO chemisorbed on silica-supported Pt, Eischens and co-workers noted that the frequency of the internal optic mode of CO depended upon intermolecular interactions between CO molecules rather than changes in the surface work function as the surface coverage was varied.³ In a subsequent study by Hammaker, Francis, and Eischens, the intermolecular

interactions were attributed to dipolar coupling and the system was modeled in that respect.⁴

Shigeishi and King have reported frequency vs. coverage data for CO on crystalline Pt(111) using infrared reflection-absorption spectroscopy. The CO stretching frequency was observed to shift from 2065 to 2100 cm^{-1} as the coverage increased from 0.6×10^{14} to 7.2×10^{14} molecules/ cm^2 .⁵ Crossley and King, using ^{13}C O on crystalline Pt(111), further verified that the observed frequency vs. coverage behavior could be attributed to dipole-dipole coupling.⁶

The dipolar coupling model used by Hamaker and co-workers⁴ and later by Crossley and King⁶ did not take into account image dipoles induced in the substrate by the adsorbed molecules. The role of the substrate was neglected except to provide adsorption sites for the CO molecules. Delanaye and co-workers,⁷ however, have since applied a molecular dipole model which includes image dipole interactions to the data reported by Shigeishi and King.⁵ Using a molecular dipole model which includes both image dipole interactions and accounts for contributions from the electronic polarizability of the adsorbed molecule, Mahan and Lucas determined that dipolar coupling could not account for the magnitude of the frequency vs. coverage shift observed with CO adsorbed on Pt(111).⁸ Those authors, however, used gas phase values for the dipole moment derivative and electronic polarizability. In addition, the frequency that is observed experimentally in the low coverage limit was used as the static surface isolation frequency, ω_0 . However, the experimentally observed value is the vibrational frequency of the adsorbed molecule including the effects of dipolar interaction with its own image. The static surface isolation frequency, ω_0 , is therefore the frequency the adsorbed molecule would have in the absence of any dipolar coupling, even with its own image.

In this work, the relationship of the molecular normal coordinates of adsorbed molecules to their associated linear combinations of real and image dipoles is discussed using group theory. A molecular dipole model, consistent with having only one possible linear combination of real and image dipoles and which takes into account the electronic polarizability of the adsorbed molecules, is developed. The inclusion of the electronic polarizability parallels Decius's³ treatment of dipolar coupling in three-dimensional crystals.⁹ Finally, this model is applied to the system, CO adsorbed on crystalline Pt(111), using the data reported by Shigeishi and King.⁵

SYMMETRY CONSIDERATIONS

A dipole adsorbed at a distance d above the surface of a perfect electrically conducting substrate will induce an image dipole in the substrate at a distance d below the surface.¹⁰ The image dipole will have the same magnitude and polarizability as the real dipole.¹¹ The symmetry of these real and image dipole systems has been previously studied by Hexter and Albrecht.² It was shown by those authors that if the molecule has the symmetry of point group S after adsorption, then the symmetry of the real-image dipole pair can be described by the direct product group,

$$\bar{S} = S \otimes \{E + R\}$$

where E is the identity operation and R is a simultaneous operation of mirror reflection in the surface combined with charge conjugation. Since the group $\{E + R\}$ is isomorphous with C_2 , the group \bar{S} is isomorphous to the direct product group:

$$H = S \otimes \{E + C_2\}$$

However, the irreducible representations of \bar{S} are not those of H, as was assumed by Hexter and Albrecht. The correlations of the groups S to \bar{S} and of S to H are different and will be illustrated using $S = C_{2v}$ as an example.

The correlation diagram of $S = C_{2v}$ to $H \leftrightarrow D_{2h} = C_{2v} \otimes \{E + C_2\}$ is shown in Fig. 1. The symbol \leftrightarrow is used to mean "isomorphous to." H and D_{2h} are isomorphous, hence we can use the same labels to denote the irreducible representations of each. Initially, only the internal coordinates, r_{1r} , r_{2r} , r_{1i} , and r_{2i} of the real and image molecules shown in Fig. 2 will be considered. The symmetric stretching modes, $q_r(A_1) = 2^{-1/2} (\Delta r_{1r} + \Delta r_{2r})$ and $q_i(A_1) = 2^{-1/2} (\Delta r_{1i} + \Delta r_{2i})$, of the real and image molecules, respectively, are combined under the symmetry operations of H to form the linear combinations, $q_+ = 2^{-1/2} (q_r + q_i)$ and $q_- = 2^{-1/2} (q_r - q_i)$. The in-phase mode, q_+ , transforms like the irreducible representation A_g whereas the out-of-phase mode, q_- , transforms like B_{1u} under the operations of H. Although the correlation of C_{2v} to D_{2h} is sufficient to describe the in-phase and out-of-phase motions of the real and image molecules, the transformations of the dipole components under D_{2h} do not properly account for the charge conjugation of the image molecule with respect to the real molecule. Charge conjugation can be accounted for, however, by allowing the dipole and Raman tensor components to transform according to the irreducible representations as shown in Fig. 1. It will now be shown that the group H does not adequately describe the system.

The internal vibrational mode $q_r(A_1)$ of an adsorbed molecule is correlated to both A_g and B_{1u} of the group H. Two distinct vibrational modes of the adsorbed molecule, q_+ and q_- , are predicted to result from one internal vibrational mode, q , of the free molecule. However, the image molecule is actually

a set of image charges induced in the substrate by the adsorbed molecule. The coordinates of the induced charges are not independent of the coordinates of the adsorbed molecule. The positions of the image charges are related to those of the molecule by the operation of mirror reflection through the plane of the surface. This symmetry plane exists not only in the equilibrium configuration but also for the displacements of the charges during a vibration. If a charge on the molecule is displaced from equilibrium by an amount $\Delta x + \Delta y + \Delta z$, for example, then the image charge, which has opposite sign, must be displaced from its equilibrium position by $R(\Delta x + \Delta y + \Delta z) = \Delta x + \Delta y - \Delta z$. The alternative displacement of the image charge by $-\Delta x - \Delta y + \Delta z$ does not take place. The symmetric stretching motion shown in Fig. 2, in which the internal coordinates of the adsorbed molecule, r_{1r} and r_{2r} , undergo displacements Δr_{1r} and Δr_{2r} must, therefore, be accompanied by the corresponding displacements, Δr_{1i} and Δr_{2i} , of the image molecule. Displacements of the image molecule in the opposite direction, $-\Delta r_{1i}$ and $-\Delta r_{2i}$, are in violation of the mirror symmetry relating the image molecule to the adsorbed molecule. The in-phase motion of the real-image molecule pair resulting from the symmetric stretch of the adsorbed molecule may be represented by the un-normalized displacement coordinate, $q_+ = (\Delta r_{1r} + \Delta r_{2r} + \Delta r_{1i} + \Delta r_{2i})$. The out-of-phase motion described by the coordinate, $q_- = (\Delta r_{1r} + \Delta r_{2r} - \Delta r_{1i} - \Delta r_{2i})$, is not allowed. Therefore, the correlation of the group $S = C_{2v}$ to the group H cannot be correct since it allows both modes, q_+ and q_- , to exist.

The correlation of $S = C_{2v}$ to the group $\bar{S} = C_{2v} \otimes \{E + R\}$ will now be considered. The presence of the antiunitary operator, R, makes the group \bar{S} a

Shubnikov type II, or grey, group. Unlike ordinary point groups (Shubnikov type I groups), the grey groups do not have a set of irreducible representations (reps). They do, however, have a set of irreducible corepresentations (coreps) whose matrices, $D_{\mathcal{H}}$, obey the equivalence relations

$$D_{\mathcal{H}}(u_1) D_{\mathcal{H}}(u_2) = D_{\mathcal{H}}(u_1 u_2) \quad (1)$$

$$D_{\mathcal{H}}(a) D_{\mathcal{H}}(u)^* = D_{\mathcal{H}}(au)$$

$$D_{\mathcal{H}}(u) D_{\mathcal{H}}(a) = D_{\mathcal{H}}(ua)$$

$$D_{\mathcal{H}}(a_1) D_{\mathcal{H}}(a_2)^* = D_{\mathcal{H}}(a_1 a_2)$$

where \underline{u} and \underline{a} are unitary and anti-unitary operations, respectively. In general, they do not obey the same multiplication rules as do the group operations.

Wigner¹² has shown that the irreducible coreps of grey groups can be derived from knowledge of the irreducible reps of the unitary subgroup, in this case the group $S = C_{2v}$. An irreducible corep of a non-unitary group is produced from the unitary subgroup by one of three ways:¹³ (a) the corep $\bar{\Gamma}$ of the group \bar{S} derived from the rep Γ of the group S will have the same dimension, (b) the rep Γ will be contained in $\bar{\Gamma}$ twice, and (c) two inequivalent reps, Γ_1 and Γ_2 , will come together in the same corep, $\bar{\Gamma}$. Cracknell and Wong have shown that if the non-unitary group is a grey group, then all the coreps will be either case (a) or case (c).¹⁴ Non-degenerate complex conjugate reps of the unitary subgroup, S , lead to case (c) coreps. Case (a) coreps will result from the remaining reps of S .

The general form of the matrices forming the corep, $\bar{\Gamma}$, are given by

$$\underline{\underline{D}}(u) = \begin{bmatrix} \Delta(u) & 0 \\ 0 & \Delta^*(R^{-1}uR) \end{bmatrix} \quad (2-A)$$

$$\underline{\underline{D}}(a) = \begin{bmatrix} 0 & \Delta(aR) \\ \Delta^*(R^{-1}a) & 0 \end{bmatrix} \quad (2-B)$$

where $\Delta(u)$ is the matrix representative of the operation u in the unitary subgroup, S . R is the anti-unitary operation, which here is a simultaneous mirror reflection through the surface combined with charge conjugation, and a is an element of the coset $\{R \otimes C_{2v}\}$. The asterisk represents the complex conjugate. All the irreducible coreps of \bar{C}_{2v} will be case (a). The coreps of \bar{C}_{2v} are shown in Fig. 3 according to the form given in (2-A) and (2-B). These coreps may be reduced using $\underline{\underline{D}}'(u) = \underline{\underline{V}}^{-1}\underline{\underline{D}}(u)\underline{\underline{V}}$ and $\underline{\underline{D}}'(a) = \underline{\underline{V}}^{-1}\underline{\underline{D}}(a)\underline{\underline{V}}^*$, where

$$\underline{\underline{V}} = 2^{-\frac{1}{2}} \begin{bmatrix} 1 & -1 \\ 1 & 1 \end{bmatrix}$$

the irreducible coreps resulting from this transformation have the form

$$\underline{\underline{D}}'(u) = \begin{bmatrix} \Delta(u) & 0 \\ 0 & \Delta(u) \end{bmatrix} \quad (3-A)$$

$$\underline{\underline{D}}'(a) = \begin{bmatrix} \Delta(aR) & 0 \\ 0 & -\Delta(aR) \end{bmatrix} \quad (3-B)$$

and are presented as 2 x 2 diagonal matrices in Fig. 4. Each of these sets of 2 x 2 matrices contain two irreducible coreps; however, both are equivalent.¹² The character table for \bar{C}_{2v} is given in Fig. 5 using four inequivalent one-dimensional irreducible coreps. The coreps with character +1 for the operation R were chosen. The correlation of $S = C_{2v}$ to $\bar{S} = C_{2v} \otimes \{E + R\}$ is shown in Fig. 6. There is a one-to-one correlation of the one-dimensional irreducible reps of S to the one-dimensional irreducible coreps of \bar{S} .

If the vector, $\langle q_r, q_i |$, is transformed by the antiunitary operator, R, according to

$$R \langle q_r, q_i | = \langle q_i, q_r |$$

where $q_r = 2^{-\frac{1}{2}}(\Delta r_{1r} + \Delta r_{2r})$ and $q_i = 2^{-\frac{1}{2}}(\Delta r_{1i} + \Delta r_{2i})$ are the symmetric stretching motions of the real and image molecules, then a suitable coordinate transforming as \bar{A}_1 under \bar{C}_{2v} is $\frac{1}{2}(q_r + q_i)$. The coordinate, q_i , may be replaced by q_r since:

$$dq_i = \frac{\partial q_i}{\partial q_r} dq_r = dq_r$$

The normal coordinate of the adsorbed molecule, q_r , is therefore a suitable normal coordinate of the real-image molecule system and will form a basis for both rep A_1 of C_{2v} and corep \bar{A}_1 and \bar{C}_{2v} .¹⁵ Regardless of how the vibrational coordinates are expressed, there will be a one-to-one correspondence between the internal modes of the adsorbed molecule and the internal modes of the real-image molecule system.

The spectroscopic activity of the normal modes of vibration for adsorbed molecules is found by examining the transformations of the dipole and polarizability components under the symmetry operations of the group \bar{S} . Any property of a system having the symmetry of the group \bar{S} must assume both its values with respect to the anti-unitary operation, R, simultaneously. A dipole perpendicular to the surface is unchanged by the operation R, whereas dipoles parallel to the surface are transformed into their negatives. Dipole components parallel to the surface must, therefore, have zero magnitude. Fig. 6 shows the vibrational correlation diagram of $S = C_{2v}$ to $\bar{S} = C_{2v} \otimes (E + R)$ with the symmetry axis (z) taken to be perpendicular to the surface.

The x and y cartesian components, as well as the xz and yz polarizability tensor elements, do not transform like any of the irreducible corepresentations of $\bar{S} = \bar{C}_{2v}$. This will be true for any S where x and y are parallel to the surface. Only the vibrational modes transforming as \bar{A}_1 under \bar{C}_{2v} are infrared active. The linear combination of real and image dipole components associated with a vibrational mode transforming as \bar{A}_1 under \bar{C}_{2v} is $\mu_r(z) + \mu_i(z)$, resulting in a non-zero dipole moment derivative perpendicular to the surface. Normal coordinates transforming as \bar{B}_1 or \bar{B}_2 under \bar{C}_{2v} have non-zero dipole moment derivatives parallel to the surface at both real and image dipole sites; however, these are equal in magnitude and opposite in direction. The net dipole moment derivatives for these coordinates are zero, as indicated by the linear combinations of dipoles, $\mu_r(x) - \mu_i(x)$ and $\mu_r(y) - \mu_i(y)$, respectively, for \bar{B}_1 and \bar{B}_2 symmetry modes. The linear combinations of dipoles, $\mu_r(z) - \mu_i(z)$, $\mu_r(x) + \mu_i(x)$, and $\mu_r(y) + \mu_i(y)$ do not transform like any of the irreducible corepresentations of \bar{C}_{2v} , and they cannot be associated with any of the vibrational modes of the adsorbed molecule.

It should be noted that although the presence of the image molecule does not require additional vibrational coordinates, it does introduce a new dipole whose position is related to the dipole of the adsorbed molecule by the operator, R.

The combination of dipoles transforming as \bar{A}_1 is $\mu_r(z) + \mu_i(z)$, not $2^{-1/2}[\mu_r(z) + \mu_i(z)]$. This fact will be used in the next section.

Using the Wigner projection operator to project symmetry adapted components of the Raman scattering tensor, α , the Raman scattering tensors transforming like the irreducible corepresentations of \bar{C}_{2v} are:¹⁶

$$\bar{A}_1 = \begin{bmatrix} \alpha_{xx} & 0 & 0 \\ 0 & \alpha_{yy} & 0 \\ 0 & 0 & \alpha_{zz} \end{bmatrix}; \quad \bar{A}_2 = \begin{bmatrix} 0 & \alpha_{xy} & 0 \\ \alpha_{yx} & 0 & 0 \\ 0 & 0 & 0 \end{bmatrix}; \quad \bar{B}_1 = \bar{B}_2 = \begin{bmatrix} 0 & 0 & 0 \\ 0 & 0 & 0 \\ 0 & 0 & 0 \end{bmatrix}$$

The absence of non-zero xz and yz tensor elements results from the dipole induced in the real molecule by an electric field being canceled by a dipole in the opposite direction induced in the image molecule. Raman activity is, therefore, associated only with those vibrational modes transforming as \bar{A}_1 or \bar{A}_2 under \bar{C}_{2v} .

Just as the group C_{2v} is the archetype of the orthorhombic, tetragonal, and cubic systems, so is the group C_3 the model subgroup of the trigonal, rhombohedral, and hexagonal systems. Therefore, the correlation of $S = C_3$ to $\bar{S} = C_3 \otimes \{E + R\}$ will now be discussed. Unlike \bar{C}_{2v} , the group \bar{C}_3 has case (c) coreps arising from the 1E and 2E reps of C_3 .¹³ The coreps which result from the application of (1-A) and (1-B) are given in Fig. 7. A reduction of the 2 x 2 matrices forming the case (a) corep, $\bar{\Gamma}(A)$, is accomplished using

$$D' = Y^{-1}DY$$

where

$$Y = 2^{-1/2} \begin{bmatrix} 1 & -1 \\ 1 & 1 \end{bmatrix}$$

Two equivalent one-dimensional coreps result from this transformation. The 2 x 2 matrices forming the coreps $\bar{\Gamma}^{(1E)}$ and $\bar{\Gamma}^{(2E)}$ are irreducible. If the matrices of $\bar{\Gamma}^{(2E)}$ are transformed according to

$$\underline{D}'(u) = \underline{V}^{-1} \underline{D}(u) \underline{V} \quad (4)$$

$$\underline{D}'(a) = \underline{V}^{-1} \underline{D}(a) \underline{V}^*$$

where \underline{V} is the unitary matrix given by

$$\underline{V} = \begin{bmatrix} 0 & i \\ -i & 0 \end{bmatrix}$$

then it is seen that $\bar{\Gamma}^{(1E)}$ and $\bar{\Gamma}^{(2E)}$ are unitarily equivalent. There are, therefore, only two inequivalent coreps for $\bar{S} = \bar{C}_3$. Neither of the equivalent coreps, $\bar{\Gamma}^{(1E)}$ or $\bar{\Gamma}^{(2E)}$, are suitable for determining the spectroscopic activities of the real-image dipole system since the x and y cartesian components have non-zero transformations. This predicts net non-zero dipole moment derivative components in the plane of the surface associated with vibrational modes transforming according to either irreducible corep, $\bar{\Gamma}^{(1E)}$ or $\bar{\Gamma}^{(2E)}$. Physical arguments presented by Pearce and Sheppard preclude this possibility.¹

The corep $\bar{\Gamma}^{(1E)}$ can be transformed into an equivalent corep, \bar{E} , by application of (4) using the transformation matrix,

$$\underline{V} = 2^{-\frac{1}{2}} \begin{bmatrix} 1 & i \\ 1 & -i \end{bmatrix}.$$

The transformations of the cartesian and Raman scattering tensor components according to the two inequivalent coreps, \bar{A} and \bar{E} , shown in Fig. 8 are consistent with the physical requirements of the real-image dipole system. Fig. 9 gives the

correlation diagram for $S = C_3$ to $\bar{S} = C_3 \otimes \{E + R\}$. The z cartesian component transforms like the \bar{A} corep of $\bar{S} = \bar{C}_3$ whereas the x and y components do not transform like any of the irreducible coreps of $\bar{S} = \bar{C}_3$. Infrared activity is, therefore, only found with those vibrational modes of the molecule which have a non-zero dipole moment derivative component perpendicular to the surface.

Two equivalent coreps of $\bar{S} = S \times \{E + R\}$ having $\underline{D}(R) = \pm \underline{D}(E)$ can always be obtained from a rep of S either by direct application of (2-A) and (2-B) or by applying (2-A) and (2-B) in conjunction with (4). These coreps will contain real matrices which satisfy (1) as well as obey the same multiplication rules as do the group operations. The properties of the real-image dipole system are described by those coreps having $\underline{D}(R) = \underline{D}(E)$.

Symmetry adapted components of the Raman scattering tensor, α , are determined as before, using the Wigner projection operator. The Raman scattering tensors transforming like the irreducible coreps of \bar{C}_3 are:

$$\bar{A} = \begin{bmatrix} \frac{1}{2}(\alpha_{xx} + \alpha_{yy}) & \frac{1}{2}(\alpha_{xy} - \alpha_{yx}) & 0 \\ -\frac{1}{2}(\alpha_{xy} - \alpha_{yx}) & \frac{1}{2}(\alpha_{xx} + \alpha_{yy}) & 0 \\ 0 & 0 & \alpha_{zz} \end{bmatrix}$$

$$\bar{E} = \begin{bmatrix} \frac{1}{2}(\alpha_{xx} - \alpha_{yy}) & \frac{1}{2}(\alpha_{xy} + \alpha_{yx}) & 0 \\ \frac{1}{2}(\alpha_{xy} + \alpha_{yx}) & -\frac{1}{2}(\alpha_{xx} - \alpha_{yy}) & 0 \\ 0 & 0 & 0 \end{bmatrix}_x$$

$$\begin{bmatrix} -\frac{1}{2}(\alpha_{xy} + \alpha_{yx}) & \frac{1}{2}(\alpha_{xx} - \alpha_{yy}) & 0 \\ \frac{1}{2}(\alpha_{xx} - \alpha_{yy}) & \frac{1}{2}(\alpha_{xy} + \alpha_{yx}) & 0 \\ 0 & 0 & 0 \end{bmatrix}_y$$

indicating Raman activity for all vibrational modes. Like $\bar{S} = \bar{C}_{2v}$, the α_{xz} and α_{yz} tensor elements do not transform like any of the irreducible coreps of $\bar{S} = \bar{C}_3$. For resonance Raman scattering, the tensor transforming as does \bar{A} need not be symmetric.^{17,18} That is, $\alpha_{xy} \neq \alpha_{yx}$. Hexter and Albrecht have suggested that the enhanced Raman scattering exhibited by some surface adsorbed molecules can be attributed to a resonance Raman effect in which the surface plasmons of the metal substrate mix with the molecular electronic states.² This provides a continuum of intermediate states for the scattering. The off-diagonal tensor elements, $\pm\frac{1}{2}(\alpha_{xy} - \alpha_{yx})$, of $\underline{g}(\bar{A})$ can then contribute to the Raman scattering. In ordinary Raman scattering, however, the approximation $\alpha_{xy} = \alpha_{yx}$ holds, and the measurable components of the Raman scattering tensor are $\alpha_{xx} + \alpha_{yy}$, α_{zz} , $\alpha_{xx} - \alpha_{yy}$, and $\alpha_{xy} + \alpha_{yx}$.

If the enhanced Raman scattering exhibited by surface adsorbed molecules is resonance Raman scattering, then the asymmetry of the Raman scattering tensor transforming as \bar{A}_2 of $\bar{S} = \bar{C}_{2v}$ could possibly be measured. The experimental scattering geometry shown in Fig. 10 allows the tensor elements, α_{xy} and α_{yx} , to be distinguished. The Raman scattering tensor for the prime coordinate system in Fig. 10 is

$$\underline{g}(\bar{A}_2) = \begin{bmatrix} 0 & \alpha_{xy} \cos \theta & 0 \\ \alpha_{yx} \cos \theta & 0 & -\alpha_{yx} \sin \theta \\ 0 & -\alpha_{xy} \sin \theta & 0 \end{bmatrix}$$

Two experiments, $z'(x'y)x'$ and $z'(yz')x'$, will give Raman scattering intensities proportional to $(\alpha_{xy} \cos \theta)^2$ and $(\alpha_{yx} \sin \theta)^2$, respectively.

If the adsorbed molecules were to form a two-dimensional lattice with the unit cell group F , the point group of the free molecules, M , must be correlated to the grey group, \bar{F} . The complete way of correlation may be represented by either of the two diagrams

$$M \rightarrow S \rightarrow F \rightarrow \bar{F}$$

or: $M \rightarrow S \rightarrow \bar{S} \rightarrow \bar{F}$

MOLECULAR DIPOLE MODEL

In order to use a rapidly converging technique for calculating lattice sums, such as the plane-wise summation method developed by Nijboer and DeWette,¹⁹ the molecules are assumed to adsorb in a perfect two-dimensional lattice. The substrate is treated as a perfect electrically conducting medium. If each unit cell is assumed to be singly occupied, it has a real dipole located at a distance d above the surface and an induced (image) dipole at a distance d below the surface. In addition, the adsorbed molecule is assumed to have only one internal optic mode of vibration, which has a frequency much higher than those of the substrate so as to be vibrationally decoupled. Extending the model to include adsorbed molecules having several internal optic modes and multiple occupied unit cells is straightforward.

Mandel and Mazur²⁰ have shown that dipolar coupling of a set of polar and polarizable molecules leads to an additional term in the potential energy of the system given by

$$\frac{1}{2} \underline{\mu}^+ \underline{T} (\underline{I} + \alpha \underline{T})^{-1} \underline{\mu} \quad (5)$$

where μ is a $3nN$ dimensional vector of the intrinsic dipole moments of the nN dipoles in the system, I is a $3nN \times 3nN$ identity matrix, α is a $3nN \times 3nN$ electronic polarizability matrix, and T is a $3nN \times 3nN$ dipole field propagation tensor. The elements of T are

$$T_{tt'} = \frac{1}{r_{tt'}^3} - \frac{3(r_{t'} - r_t)(r_{t'} - r_t)}{r_{tt'}^5}$$

if $t \neq t'$, where $r_{tt'}$ is the distance between dipoles at positions t and t' , and $T_{tt'} = 0$ if $t = t'$. N is the number of unit cells and n is the number of dipoles per unit cell. For each adsorbed molecule, there are two dipoles per unit cell, one being the intrinsic dipole associated with the molecule and the other being the image dipole induced in the substrate.

The potential energy of the system may be written through its quadratic terms as

$$2V = q^T \omega_0^2 q + \mu^T (I + \alpha T)^{-1} \mu \quad (6)$$

where q is an N -dimensional vector of mass-weighted molecular normal coordinates of the adsorbed molecules and ω_0^2 is an $N \times N$ diagonal matrix of the squared frequencies of the molecular normal modes in the absence of dipolar coupling. Both real and image dipoles are expanded in terms of the same molecular normal coordinates, q_t :

$$\begin{aligned} \mu_{\beta\tau r} &= \mu_{\beta\tau r}^0 + \frac{\partial \mu_{\beta\tau r}}{\partial q_t} q_t + \dots \\ \mu_{\beta\tau i} &= \mu_{\beta\tau i}^0 + \frac{\partial \mu_{\beta\tau i}}{\partial q_t} q_t + \dots \end{aligned} \quad (7)$$

where the subscripts r and i denote real and image dipoles, respectively, in unit cell τ and β is a cartesian component of the dipoles. Substituting the terms linear in q for μ in (2), the potential energy may be expressed as

$$2V = q_{\alpha}^+ \omega_{\alpha}^2 q_{\alpha} + q_{\alpha}^+ M_{\alpha\beta}^+ T_{\alpha\beta} (I_{\alpha\beta} + \alpha_{\alpha\beta} T_{\alpha\beta})^{-1} M_{\alpha\beta} q_{\alpha} (\partial\mu/\partial q)^2 \quad (8)$$

where $M_{\alpha\beta}$ is a $6N \times 3N$ matrix relating the real and image dipole components to the molecular normal coordinates. The elements of $M_{\alpha\beta}$ are:

$$\begin{aligned} M_{\beta\gamma\tau\tau'} &= \begin{bmatrix} 1 \\ 1 \end{bmatrix} && \text{if } \beta = \gamma = z, \tau = \tau' \\ &= \begin{bmatrix} 1 \\ -1 \end{bmatrix} && \text{if } \beta = \gamma = x \text{ or } y, \tau = \tau' \\ &= \begin{bmatrix} 0 \\ 0 \end{bmatrix} && \text{if } \beta \neq \gamma \text{ or } \tau \neq \tau' \end{aligned}$$

The molecular normal coordinates, q , may be transformed into translationally symmetrized normal coordinates, Q , by the transformation

$$Q_{\alpha} = X_{\alpha\tau} q_{\alpha}$$

where

$$X_{\alpha\tau} = (1/N)^{1/2} e^{-i\mathbf{k} \cdot \mathbf{x}(\tau)}$$

and where \mathbf{k} is the wavevector and $\mathbf{x}(\tau)$ is the position vector of unit cell τ .

The potential energy may now be written as

$$2V = Q_{\alpha}^+ \omega_{\alpha}^2 Q_{\alpha} + Q_{\alpha}^+ M_{\alpha\beta}^+ S_{\alpha\beta} (I_{\alpha\beta} + \alpha_{\alpha\beta} S_{\alpha\beta})^{-1} M_{\alpha\beta} Q_{\alpha} (\partial\mu/\partial q)^2 \quad (9)$$

where

$$S_{\alpha\beta} = X_{\alpha\tau}^+ T_{\alpha\beta} X_{\alpha\tau}^{-1} .$$

The S_{kk} matrix is block diagonal in k with the $S_{kk\beta\beta}$ block being given by

$$\begin{bmatrix} S_{rr} & S_{ri} \\ S_{ir} & S_{ii} \end{bmatrix}_{kk\beta\beta} = \begin{bmatrix} S_{rr} & S_{ri} \\ S_{ri} & S_{rr} \end{bmatrix}_{kk\beta\beta}$$

where the subscripts r and i refer to the real and image dipoles, respectively. If the dipole moment derivative associated with the molecular normal mode, q , of the adsorbed molecule is non-zero and normal to the surface, taken here to be the z direction, then the frequency of Q_k will be given by:

$$\omega(k)^2 = \omega_0^2 + \frac{2(S_{rr} + S_{ri})_{kk\beta\beta} (\partial\mu/\partial q)^2}{1 + \alpha(S_{rr} + S_{ri})_{kk\beta\beta}} \quad (10)$$

For x or y components, taken here to be parallel to the surface, the frequency will be given by:

$$\omega(k)^2 = \omega_0^2 + \frac{2(S_{rr} - S_{ri})_{kk\beta\beta} (\partial\mu/\partial q)^2}{1 + \alpha(S_{rr} - S_{ri})_{kk\beta\beta}} \quad (11)$$

The factor of 2 found in the dipole shift term in (10) and (11) arises from expanding both the real and image dipoles in terms of the same molecular normal coordinates.

If a separate normal coordinate is assigned to the image dipole and the system treated as though there are two molecules per unit cell, then the linear combinations

$$Q_{k+} = (1/2)^{1/2} (Q_{kr} + Q_{ki})$$

$$Q_{k-} = (1/2)^{1/2} (Q_{kr} - Q_{ki})$$

must be taken. This gives two frequencies:

$$\omega_+^2 = \omega_0^2 + \frac{(S_{rr} + S_{ri})_{kk\beta\beta} (\partial\mu/\partial q)^2}{1 + \alpha(S_{rr} + S_{ri})_{kk\beta\beta}} \quad (12-A)$$

$$\omega_-^2 = \omega_0^2 + \frac{(S_{rr} - S_{ri})_{kk\beta\beta} (\partial\mu/\partial q)^2}{1 + \alpha(S_{rr} - S_{ri})_{kk\beta\beta}} \quad (12-B)$$

This treatment is consistent with a correlation of the group S to the group $H = S \otimes \{E \oplus C_2\}$. Previous authors have used this method and recognized that if z dipole components are used then only Q_{k+} is physically allowed whereas for x or y dipole components only Q_{k-} is allowed.^{7,8} The remaining modes were discarded. An objection to this is that if two molecular normal coordinates, q_r and q_i , are coupled by dipolar interaction then both linear combinations, Q_{k+} and Q_{k-} , should be allowed. These two linear combinations may have different frequencies and may correlate to different irreducible representations of H. The result of this method is not equivalent to the result found by expanding both real and image dipoles in terms of the same molecular normal coordinate. If two molecular normal coordinates, q_r and q_i , are used then the frequency shift is only half that found when both dipoles are expanded in terms of the same molecular normal coordinate.

APPLICATION TO CO ON Pt(111)

Shigeishi and King have reported the frequency as a function of surface coverage for carbon monoxide on the (111) face of crystalline platinum using infrared reflection-absorption spectroscopy.⁵ This same data was used by Delanaye and co-workers⁷ in a dipole calculation similar to the one reported here. However, these authors neglected the electronic polarizability, and also assigned a separate normal coordinate to the image dipole.

In order to use the rapidly converging plane-wise lattice sum procedure developed by DeWette and Schacher,²¹ the adsorbed molecules must assume a two-dimensional lattice. Although this might possibly be achieved in the full coverage limit, it will not be the case at intermediate coverage.

Two different methods of calculating lattice sums at intermediate coverage are considered here. The first method is to determine an effective lattice constant using

$$a = (10^{16}/n \sin 60)^{1/2} \quad (13)$$

where n is the number of molecules per square centimeter of surface and a is the hexagonal lattice constant in angstroms. The lattice sums are given by

$$S_{rr} = \frac{1}{a^3} \sum_j \frac{1}{r_{oj}^3} = \frac{1}{a^3} (11.03418) \quad (14-A)$$

$$S_{ri} = \frac{8\pi^2}{\sqrt{3} a^3} \sum_{n_1 n_2} |h_{n_1 n_2}| \exp(-4\pi h_{n_1 n_2} d/a) \quad (14-B)$$

where r_{oj} is the distance of the j^{th} molecule from the origin molecule, d is the distance of the dipole to the surface, and $h_{n_1 n_2}$ is the two-dimensional reciprocal lattice vector. The summation is over a reciprocal lattice with a basis length of $2/\sqrt{3} a$.

The second method is to take the lattice sum for some full coverage lattice and multiply it by the coverage fraction. For dipoles oriented perpendicular to the surface, the lattice sum calculated in this manner is equivalent to assigning each molecule a probability equal to the coverage fraction for being at the site. The lattice sums for this method are given by

$$S_{rr} = \frac{X}{a_0^3} (11.03418) \quad (15-A)$$

$$S_{ri} = \frac{8\pi^2 X}{\sqrt{3} a_0^3} \sum_{n_1 n_2} |h_{n_1 n_2}| \left[\exp(-4\pi h_{n_1 n_2} d/a_0) - \frac{2(1-X)}{(2d)^3} \right] \quad (15-B)$$

where a_0 is the full coverage hexagonal lattice constant and X is the coverage fraction. The second term in (15-B) takes into account the fact that the image dipole in the origin unit cell is always present. This method has been used by Mahan and Lucas⁸ and also by Bennett.²² Mahan and Lucas presented statistical arguments to support this method of obtaining lattice sums at intermediate coverage.

RESULTS

Eight cases are now considered to show the effects of including image dipoles, the electronic polarizability, and the two different methods of lattice summation. Setting $\alpha = 0$ in (10) gives the expression arrived at if the electronic polarizability is neglected. The distance of the dipole to the surface appears only in the real-image dipole lattice sum, S_{ri} , and is not a parameter when image dipoles are neglected. Omitting the factor of 2 and S_{ri} from (10) allows the equation to be applied to cases where image dipoles are neglected. Using

$|\partial\mu/\partial q|$, α , d , and ω_0 as adjustable parameters, a least squares fit of (10) to the data of Shigeishi and King⁵ produced the values listed in Table 1. The parameters in those columns labeled "lattice sum method 1" were calculated by assigning an effective lattice constant for intermediate coverage using (13), (14-A) and (14-B). The intermediate coverage lattice sums used to determine the parameters in the columns labeled "lattice sum method 2" were calculated according to (15-A) and (15-B) with the full coverage hexagonal lattice constant taken to be the same as that of Pt(111), 2.77 Å. Blank values in the table indicate that those parameters were not applicable to that particular case.

The frequency vs. coverage curves shown in Fig. 11 were calculated using the values in Columns 1 and 2 of Table 1. These curves are representative of those obtained by using the values in the remaining columns in Table 1.[†] Regardless of which lattice summation method is used or, whether or not image dipoles are considered, the agreement of the dipolar coupling model with the experimental data is greatly improved by the inclusion of the electronic polarizability. The slope of the frequency vs. coverage curve, as seen in Fig. 14, decreases with increasing surface coverage if the electronic polarizability is included, which is the experimentally observed behavior. With the exception of the values of the parameters listed in Column 8 of Table 1, which predicts a linear dependence of frequency on coverage, the slope of the frequency vs. coverage curves increases with increasing coverage if the electronic polarizability is neglected. This is contrary to the experimental results.

[†]The error bars on the experimental points in Fig. 3 represent these authors' ability to take the points from the graph reported by Shigeishi and King, they do not reflect the precision of the measurements by those authors.

The values of the parameters in Columns 1 and 3 of Table 1 give the best overall agreement with the experimental data. The dipole moment derivative, electronic polarizability, and the frequency, ω_0 , of adsorbed CO without any dipolar coupling are all lower using the second method of lattice summation as compared to the first. This is due to a contribution to the lattice sum from dipoles at a distance a_0 from the origin dipole even at low coverage when the second method of lattice summation is used. Benedict and co-workers²³ reported the dipole moment derivative of CO in the gas phase as $91 \text{ cm}^{3/2} \text{ sec}^{-1}$. This value is lower than that calculated in either Columns 1 or 3 of Table 1; however, there is no reason to assume that the dipole moment derivative for surface-adsorbed CO is the same as its gas phase value. The dipole moment derivative calculated here represents that component perpendicular to the surface. Its magnitude supports the previous assumption that the CO molecules are bonded perpendicular to the surface. It is usually assumed that CO frequencies in the range 1800 to 1920 cm^{-1} are due to a bridged structure whereas frequencies above 2000 cm^{-1} are attributed to linear metal-CO structures.²⁴ The experimental frequency observed for adsorbed CO, 2063 to 2100 cm^{-1} , indicates that the CO molecule is linearly bonded to one metal atom. LEED studies by Ertl and co-workers²⁵ found that at coverages up to 5×10^{14} molecules cm^{-2} , the adsorbed molecules have a $(\sqrt{3} \times \sqrt{3})R30^\circ$ structure in which the CO molecules are linearly bonded on top of the Pt atoms. At higher coverage, a $C(4 \times 2)$ structure was observed which allows half the CO molecules to be bridge bonded. The data reported by Shigeishi and King⁵ covered the range 0 to 7×10^{14} molecules cm^{-2} . Their data was shown in this work to fit a model having only one set of geometric and molecular parameters. This indicates that the adsorption site is not of primary importance.

Applequist and co-workers²⁶ reported the electronic polarizability of CO along the internuclear axis as $2.6 \pm 0.1 \text{ \AA}^3$. Both values of this parameter in Columns 1 and 3 of Table 1 are greater than 2.6 \AA^3 . The value of 3.5 \AA^3 , which results from the second method of lattice summation, is closer to that reported by Applequist, *et al.*

The observed frequency, ω_s , for the adsorbed molecule in the low coverage limit, $\omega_s = \lim_{x \rightarrow 0} \omega$, includes the dipolar interaction of the surface isolated molecule with its own image. Crossley and King reported this to be 2063 cm^{-1} .⁶ This is in good agreement with the values 2065 and 2062 cm^{-1} in Columns 1 and 3 of Table 1, respectively. At low coverage, the real dipole-image dipole interaction is dominant. These inter-planar forces are attractive, and they lower the frequency below the frequency, ω_0 , expected for adsorbed molecules without dipolar coupling. At high coverage, the repulsive forces between dipoles in the same plane become dominant, which raises the observed frequency above ω_0 .

The distance of the dipole to the surface is calculated to be too low if the CO molecule is assumed to be bonded to only one Pt atom and oriented perpendicular to the surface. Metal-carbonyl bond distances are on the order of $1.8 - 2.0 \text{ \AA}$.^{27,28} Although the value of 1.86 \AA in Column 1 of Table 1 is within this range, the location of the point dipole would have to be on the carbon atom, rather than at some position intermediate between the carbon and oxygen atoms. The calculated distances may not, however, be too small if the CO molecule is assumed to be bridged through the carbon atom to two Pt atoms. Alternatively, the "effective surface plane" could be above the plane containing the Pt atoms. The image atom is only a charge located at some point within the substrate. Its position is determined by mirror symmetry through the plane of the "surface" which does not have to coincide with the plane containing the outermost Pt atoms.

The frequency vs. coverage curves obtained using the parameter values in Columns 5 and 7 of Table 1, which neglect image dipoles, give excellent fits to the experimental data points. This does, however, require unacceptably large values of $|\partial\mu/\partial q|$ and, using the first method of lattice summation, the predicated electronic polarizability is also much too large.

The symmetry of the real-plus-image molecule system is described by the group $\bar{S} = S \otimes \{E + R\}$, where S is the site symmetry of the adsorbed molecule. The group \bar{S} is a Shubnikov type II point group as a result of the operation R , which is the operation of mirror reflection through the plane of the surface combined with a simultaneous charge conjugation, being antiunitary. The group \bar{S} does not have a set of reps, however, it does have a set of coreps with matrices defined by a more complex set of relationships. Real reps of S have a one-to-one correlation to the coreps of \bar{S} . Complex conjugate pairs of one-dimensional reps of S correlate to a common two-dimensional corep of \bar{S} . There is, therefore, a one-to-one correlation of the vibrational modes of the adsorbed molecule to the vibrational modes of the molecule-plus-image system.

DISCUSSION

The spectroscopic activity observed by Pearce and Sheppard¹ for the normal modes of vibration of adsorbed molecules can be supported using symmetry arguments. Only those vibrational modes having non-zero dipole moment derivative components perpendicular to the surface can be infrared active if image dipoles are important in the system being studied. The symmetry properties of the real-image dipole system has been shown to be consistent with having only one linear combination of dipoles associated with each molecular normal coordinate of the adsorbed

molecule. A consequence of having two dipoles associated with one molecule is that the dipolar coupling is enhanced by a factor of 2. A further enhancement of the dipolar coupling arises if the second method of lattice summation discussed here is used. This result is due to the lattice sum being larger for a particular surface coverage using the second method of lattice summation as opposed to the first method considered in this paper.

The calculated parameters using the second method of lattice summation depend not only upon the number of molecules per two-dimensional unit cell but also on the full coverage lattice constant, a_0 . The parameter values may change somewhat if some other two-dimensional unit cell is chosen, rather than the one used in this work, but there is little doubt that the frequency vs. coverage behavior of the internal optic mode of CO on Pt(111) is due to dipolar coupling.

It has been demonstrated that inclusion of the electronic polarizability is necessary in order to reproduce the experimentally observed frequency vs. coverage behavior using the dipolar coupling model. The primary differences found by including image dipoles as opposed to neglecting them are that the dipole moment derivative, electronic polarizability, and static surface isolation frequency, ω_0 , required to satisfy the experimental data are different. The ability to fit the frequency vs. coverage data is not especially affected.

REFERENCES

1. H. A. Pearce and N. Sheppard, Surf. Sci. 59, 205 (1976).
2. R. M. Hexter and M. G. Albrecht, Spectrochim. Acta. 35A, 233 (1979).
3. R. P. Eischens, S. A. Francis, and W. A. Pliskin, J. Phys. Chem. 60, 194 (1956).
4. R. M. Hammaker, S. A. Francis, and R. P. Eischens, Spectrochimica Acta 21, 1295 (1965).
5. R. A. Shigeishi and D. A. King, Surf. Sci. 58, 379 (1976).
6. A. Crossley and D. A. King, Surf. Sci. 68, 528 (1977).
7. F. Delanaye, A. A. Lucas and G. D. Mahan, Proc. 7th Intern. Vac. Cong. & 3rd Intern. Conf. Solid Surfaces (Vienna 1977).
8. G. D. Mahan and A. A. Lucas, J. Chem. Phys. 68, 1344 (1978).
9. J. C. Decius, J. Chem. Phys. 49, 1387 (1968).
10. J. D. Jackson, Classical Electrodynamics, John Wiley & Sons, New York (1962).
11. S. Efrima and H. Metiu, J. Chem. Phys. 70, 1602 (1979).
12. E. P. Wigner, Group Theory and Its Application to the Quantum Mechanics of Atomic Spectra (Academic Press, New York, 1959).
13. C. T. Bradley and A. P. Cracknell, The Mathematical Theory of Symmetry in Solids, Oxford (1972), Chapter 7.
14. A. P. Cracknell and K. C. Wong, Aust. J. Phys. 20, 173 (1967).
15. A. P. Cracknell, J. Phys. C. 2, 500 (1969).
16. R. Claus, L. Merten, J. Brandmüller, Springer Tracts in Modern Physics: Light Scattering by Phonon-Polaritons, V75, p. 23-40 (Springer-Verlag, New York, 1975).
17. O. S. Mortensen and J. A. Koningstein, J. Chem. Phys. 48, 3971 (1968).
18. J. A. Koningstein, Chem. Phys. Lett. 2, 31 (1968).
19. B. R. A. Nijboer and F. W. DeWette, Physica 24, 422 (1958).
20. M. Mandel and P. Mazur, Physica 24, 116 (1958).
21. E. W. DeWette and G. E. Schacher, Phys. Rev. 137, A78 (1965).

22. A. J. Bennett, *J. Chem. Phys.* 49, 1340 (1968).
23. W. S. Benedict, R. Herman, G. E. Moore, and S. Silverman, *Astrophys. J.* 135, 277 (1962).
24. G. E. Thomas and W. H. Weinberg, *J. Chem. Phys.* 70, 1437 (1979).
25. G. Ertl, M. Neumann, and K. M. Streit, *Surf. Sci.* 64, 393 (1977).
26. J. Applequist, J. R. Carl, and K. K. Fung, *J. Amer. Chem. Soc.* 94, 2952 (1972).
27. A. F. Wells, Structural Inorganic Chemistry, 4th edition, Clarendon Press, Oxford (1975).
28. I. D. Brown, et. al., Bond Index to the Determinations of Inorganic Crystal Structures, 1969 to 1977.

Figure Captions

- Figure 1. Correlation of the group C_{2v} to the direct product group, $H \leftrightarrow D_{2h} = C_{2v} \otimes \{E + C_2\}^{2v}$.
- Figure 2. Symmetric stretching motion of real-plus-image molecule system having point group symmetry $\overline{C}_{2v} = C_{2v} \otimes \{E + R\}$.
- Figure 3. Reducible coreps of the group $\overline{C}_{2v} = C_{2v} \otimes \{E + R\}$ formed by application of (2-A) and (2-B).
- Figure 4. Reduced coreps of the group $\overline{C}_{2v} = C_{2v} \otimes \{E + R\}$.
- Figure 5. The four inequivalent irreducible corepresentations of the group $\overline{C}_{2v} = C_{2v} \otimes \{E + R\}$.
- Figure 6. Correlation diagram for adsorbed molecule symmetry, C_{2v} , to the real-plus-image symmetry, $\overline{C}_{2v} = C_{2v} \otimes \{E + R\}$.
- Figure 7. Coreps of the group $\overline{C}_3 = C_3 \otimes \{E + R\}$ formed by application of (2-A) and (2-B).
- Figure 8. The two inequivalent irreducible corepresentations of the group $\overline{C}_3 = C_3 \otimes \{E + R\}$.
- Figure 9. Correlation diagram for C_3 to $\overline{C}_3 = C_3 \otimes \{E + R\}$.
- Figure 10. Proposed geometry to determine antisymmetric Raman scattering tensor elements of $\overline{C}_{2v} = C_{2v} \otimes \{E + R\}$.
- Figure 11. Graph of frequency as a function of coverage for CO/Pt(III) using equation 10. The parameter values used to calculate the solid curve are given in column 1 of table 1 whereas the values listed in column 2 were used to calculate the dotted curve.

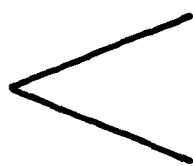
Table Captions

Table 1. Table of parameters used to fit the experimental data to the molecular dipole model.

C_{2v}

H ↔ D_{2h}

A₁

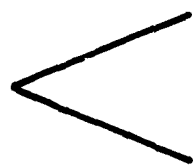


A_g Z, XX, YY, ZZ

Z(R)+Z(I)

B_{1u} Z(R)-Z(I)

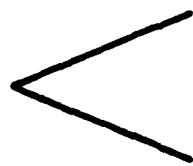
A₂



B_{1g} XY

A_u

B₁

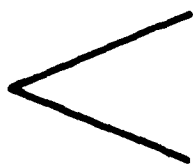


B_{2g} X, XZ

X(R)+X(I)

B_{3u} X(R)-X(I)

B₂



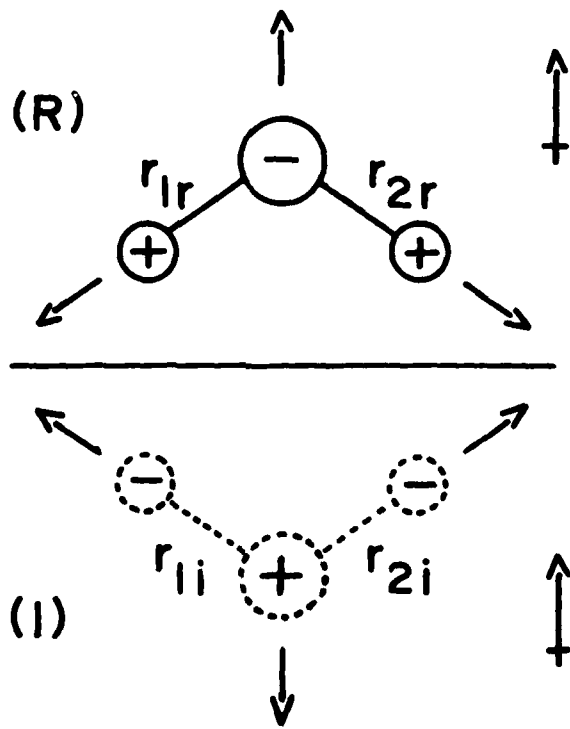
B_{3g} Y, YZ

Y(R)+Y(I)

B_{2u} Y(R)-Y(I)

$$\bar{A}_1 \quad Z$$

$$Z(R) + Z(I) \quad x$$



\bar{C}_{2v}	E	C_2	σ_{xz}	σ_{yz}	\bar{R}	\bar{C}_2	$\bar{\sigma}_{xz}$	$\bar{\sigma}_{yz}$
\bar{A}_1	$\begin{bmatrix} 1 & 0 \\ 0 & 1 \end{bmatrix}$	$\begin{bmatrix} 1 & 0 \\ 0 & 1 \end{bmatrix}$	$\begin{bmatrix} 1 & 0 \\ 0 & 1 \end{bmatrix}$	$\begin{bmatrix} 1 & 0 \\ 0 & 1 \end{bmatrix}$	$\begin{bmatrix} 0 & 1 \\ 1 & 0 \end{bmatrix}$	$\begin{bmatrix} 0 & 1 \\ 1 & 0 \end{bmatrix}$	$\begin{bmatrix} 0 & 1 \\ 1 & 0 \end{bmatrix}$	$\begin{bmatrix} 0 & 1 \\ 1 & 0 \end{bmatrix}$
\bar{A}_2	$\begin{bmatrix} 1 & 0 \\ 0 & 1 \end{bmatrix}$	$\begin{bmatrix} 1 & 0 \\ 0 & 1 \end{bmatrix}$	$\begin{bmatrix} -1 & 0 \\ 0 & -1 \end{bmatrix}$	$\begin{bmatrix} -1 & 0 \\ 0 & -1 \end{bmatrix}$	$\begin{bmatrix} 0 & 1 \\ 1 & 0 \end{bmatrix}$	$\begin{bmatrix} 0 & 1 \\ 1 & 0 \end{bmatrix}$	$\begin{bmatrix} 0 & -1 \\ -1 & 0 \end{bmatrix}$	$\begin{bmatrix} 0 & -1 \\ -1 & 0 \end{bmatrix}$
\bar{B}_1	$\begin{bmatrix} 1 & 0 \\ 0 & 1 \end{bmatrix}$	$\begin{bmatrix} -1 & 0 \\ 0 & -1 \end{bmatrix}$	$\begin{bmatrix} 1 & 0 \\ 0 & 1 \end{bmatrix}$	$\begin{bmatrix} -1 & 0 \\ 0 & -1 \end{bmatrix}$	$\begin{bmatrix} 0 & 1 \\ 1 & 0 \end{bmatrix}$	$\begin{bmatrix} 0 & -1 \\ -1 & 0 \end{bmatrix}$	$\begin{bmatrix} 0 & 1 \\ 1 & 0 \end{bmatrix}$	$\begin{bmatrix} 0 & -1 \\ -1 & 0 \end{bmatrix}$
\bar{B}_2	$\begin{bmatrix} 1 & 0 \\ 0 & 1 \end{bmatrix}$	$\begin{bmatrix} -1 & 0 \\ 0 & -1 \end{bmatrix}$	$\begin{bmatrix} -1 & 0 \\ 0 & -1 \end{bmatrix}$	$\begin{bmatrix} 1 & 0 \\ 0 & 1 \end{bmatrix}$	$\begin{bmatrix} 0 & 1 \\ 1 & 0 \end{bmatrix}$	$\begin{bmatrix} 0 & -1 \\ -1 & 0 \end{bmatrix}$	$\begin{bmatrix} 0 & -1 \\ -1 & 0 \end{bmatrix}$	$\begin{bmatrix} 0 & 1 \\ 1 & 0 \end{bmatrix}$

\bar{C}_{2v}	E	C_2	σ_{xz}	σ_{yz}	\bar{R}	\bar{C}_2	$\bar{\sigma}_{xz}$	$\bar{\sigma}_{yz}$
\bar{A}_1	$\begin{bmatrix} 1 & 0 \\ 0 & 1 \end{bmatrix}$	$\begin{bmatrix} 1 & 0 \\ 0 & 1 \end{bmatrix}$	$\begin{bmatrix} 1 & 0 \\ 0 & 1 \end{bmatrix}$	$\begin{bmatrix} 1 & 0 \\ 0 & 1 \end{bmatrix}$	$\begin{bmatrix} 1 & 0 \\ 0 & -1 \end{bmatrix}$	$\begin{bmatrix} 1 & 0 \\ 0 & -1 \end{bmatrix}$	$\begin{bmatrix} 1 & 0 \\ 0 & -1 \end{bmatrix}$	$\begin{bmatrix} 1 & 0 \\ 0 & -1 \end{bmatrix}$
\bar{A}_2	$\begin{bmatrix} 1 & 0 \\ 0 & 1 \end{bmatrix}$	$\begin{bmatrix} 1 & 0 \\ 0 & 1 \end{bmatrix}$	$\begin{bmatrix} -1 & 0 \\ 0 & -1 \end{bmatrix}$	$\begin{bmatrix} -1 & 0 \\ 0 & -1 \end{bmatrix}$	$\begin{bmatrix} 1 & 0 \\ 0 & -1 \end{bmatrix}$	$\begin{bmatrix} 1 & 0 \\ 0 & -1 \end{bmatrix}$	$\begin{bmatrix} -1 & 0 \\ 0 & 1 \end{bmatrix}$	$\begin{bmatrix} -1 & 0 \\ 0 & 1 \end{bmatrix}$
\bar{B}_1	$\begin{bmatrix} 1 & 0 \\ 0 & 1 \end{bmatrix}$	$\begin{bmatrix} -1 & 0 \\ 0 & -1 \end{bmatrix}$	$\begin{bmatrix} 1 & 0 \\ 0 & 1 \end{bmatrix}$	$\begin{bmatrix} -1 & 0 \\ 0 & -1 \end{bmatrix}$	$\begin{bmatrix} 1 & 0 \\ 0 & -1 \end{bmatrix}$	$\begin{bmatrix} -1 & 0 \\ 0 & 1 \end{bmatrix}$	$\begin{bmatrix} 1 & 0 \\ 0 & -1 \end{bmatrix}$	$\begin{bmatrix} -1 & 0 \\ 0 & 1 \end{bmatrix}$
\bar{B}_2	$\begin{bmatrix} 1 & 0 \\ 0 & 1 \end{bmatrix}$	$\begin{bmatrix} -1 & 0 \\ 0 & -1 \end{bmatrix}$	$\begin{bmatrix} -1 & 0 \\ 0 & -1 \end{bmatrix}$	$\begin{bmatrix} 1 & 0 \\ 0 & 1 \end{bmatrix}$	$\begin{bmatrix} 1 & 0 \\ 0 & -1 \end{bmatrix}$	$\begin{bmatrix} -1 & 0 \\ 0 & 1 \end{bmatrix}$	$\begin{bmatrix} -1 & 0 \\ 0 & 1 \end{bmatrix}$	$\begin{bmatrix} 1 & 0 \\ 0 & -1 \end{bmatrix}$

\bar{C}_{2v}	E	C_2	σ_{xz}	σ_{yz}	\bar{R}	\bar{C}_2	$\bar{\sigma}_{xz}$	$\bar{\sigma}_{yz}$
$\bar{A}_1(+)$	1	1	1	1	1	1	1	1
$\bar{A}_2(+)$	1	1	-1	-1	1	1	-1	-1
$\bar{B}_1(+)$	1	-1	1	-1	1	-1	1	-1
$\bar{B}_2(+)$	1	-1	-1	1	1	-1	-1	1

	REAL SITE		GREY SITE	
	SYMMETRY		SYMMETRY	
	C_{2v}		\bar{C}_{2v}	
Z XX, YY, ZZ	A_1	————	\bar{A}_1	Z, XX, YY, ZZ Z(R)+Z(I)
XY	A_2	————	\bar{A}_2	XY
X, XZ	B_1	————	\bar{B}_1	X(R)-X(I)
Y, YZ	B_2	————	\bar{B}_2	Y(R)-Y(I)

\bar{C}_3	<u>E</u>	<u>C₃</u>	<u>C₃²</u>	<u>R</u>	<u>\bar{C}_3</u>	<u>\bar{C}_3^2</u>
\bar{A}	$\begin{bmatrix} 1 & 0 \\ 0 & 1 \end{bmatrix}$	$\begin{bmatrix} 1 & 0 \\ 0 & 1 \end{bmatrix}$	$\begin{bmatrix} 1 & 0 \\ 0 & 1 \end{bmatrix}$	$\begin{bmatrix} 0 & 1 \\ 1 & 0 \end{bmatrix}$	$\begin{bmatrix} 0 & 1 \\ 1 & 0 \end{bmatrix}$	$\begin{bmatrix} 0 & 1 \\ 1 & 0 \end{bmatrix}$
${}^1\bar{E}$	$\begin{bmatrix} 1 & 0 \\ 0 & 1 \end{bmatrix}$	$\begin{bmatrix} \epsilon & 0 \\ 0 & \epsilon^* \end{bmatrix}$	$\begin{bmatrix} \epsilon^* & 0 \\ 0 & \epsilon \end{bmatrix}$	$\begin{bmatrix} 0 & 1 \\ 1 & 0 \end{bmatrix}$	$\begin{bmatrix} 0 & \epsilon \\ \epsilon^* & 0 \end{bmatrix}$	$\begin{bmatrix} 0 & \epsilon^* \\ \epsilon & 0 \end{bmatrix}$
${}^2\bar{E}$	$\begin{bmatrix} 1 & 0 \\ 0 & 1 \end{bmatrix}$	$\begin{bmatrix} \epsilon^* & 0 \\ 0 & \epsilon \end{bmatrix}$	$\begin{bmatrix} \epsilon & 0 \\ 0 & \epsilon^* \end{bmatrix}$	$\begin{bmatrix} 0 & 1 \\ 1 & 0 \end{bmatrix}$	$\begin{bmatrix} 0 & \epsilon^* \\ \epsilon & 0 \end{bmatrix}$	$\begin{bmatrix} 0 & \epsilon \\ \epsilon^* & 0 \end{bmatrix}$

$$\begin{array}{ccccccc}
 \bar{C}_3 & E & C_3 & C_3^2 & R & \bar{C}_3 & \bar{C}_3^2 \\
 \bar{A} & 1 & 1 & 1 & 1 & 1 & 1
 \end{array}$$

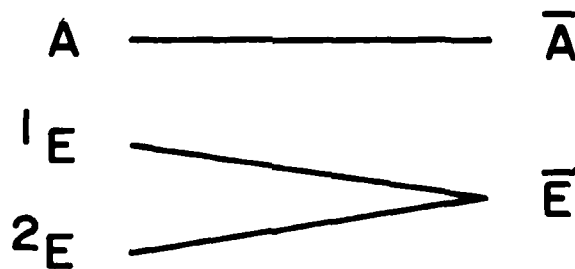
$$\bar{E} \quad \begin{bmatrix} 1 & 0 \\ 0 & 1 \end{bmatrix} \begin{bmatrix} -1/2 & -\sqrt{3}/2 \\ \sqrt{3}/2 & -1/2 \end{bmatrix} \begin{bmatrix} -1/2 & \sqrt{3}/2 \\ -\sqrt{3}/2 & -1/2 \end{bmatrix} \begin{bmatrix} 1 & 0 \\ 0 & 1 \end{bmatrix} \begin{bmatrix} -1/2 & -\sqrt{3}/2 \\ \sqrt{3}/2 & -1/2 \end{bmatrix} \begin{bmatrix} -1/2 & \sqrt{3}/2 \\ -\sqrt{3}/2 & -1/2 \end{bmatrix}$$

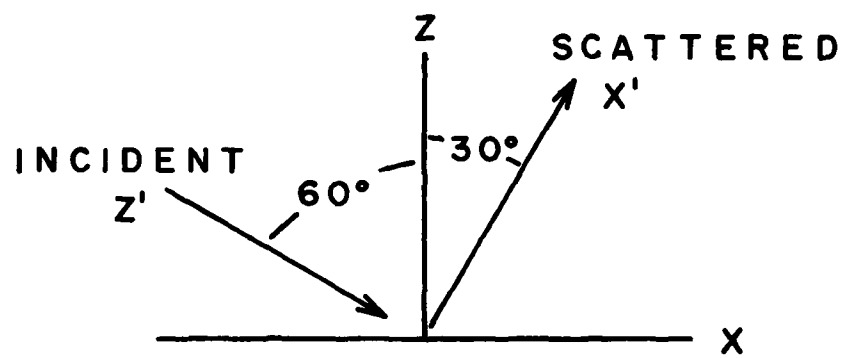
REAL SITE
SYMMETRY

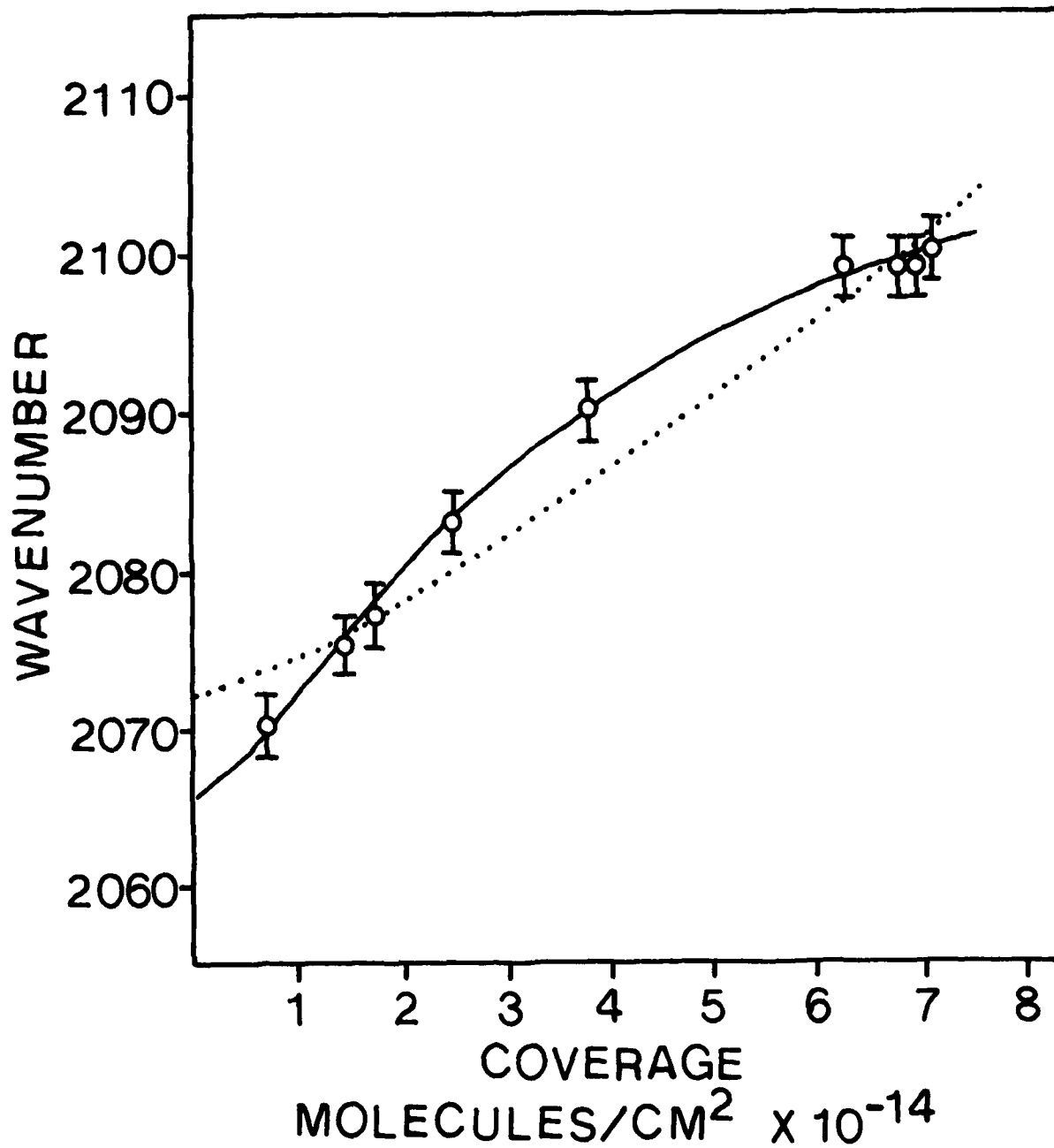
GREY SITE
SYMMETRY

C_3

\bar{C}_3







	<u>Real + Image Dipoles</u>				<u>Real Dipoles Only</u>			
	<u>Lattice Sum</u>		<u>Lattice Sum</u>		<u>Lattice Sum</u>		<u>Lattice Sum</u>	
	<u>Method 1</u>		<u>Method 2</u>		<u>Method 1</u>		<u>Method 2</u>	
$ \partial\mu/\partial q (\text{cm}^{3/2} \text{ sec}^{-1})$	141	102	120	94	327	157	195	139
$\omega_o (\text{cm}^{-1})$	2080	2079	2076	2075	2066	2074	2065	2069
$d (\text{\AA})$	1.86	1.74	1.62	1.77	--	--	--	--
$\alpha (\text{\AA}^3)$	7.0	--	3.5	--	15.6	--	3.1	--
$\omega_s (\text{cm}^{-1})$	2065	2072	2062	2068	2066	2074	2065	2069
sum of squared residuals	2.8	56	4.2	34	1.9	76	7.0	34